SCA2003-28: ANISOTROPY OF RESISTIVITY IN OIL BEARING THIN-BEDDED FORMATION: EXPERIMENT AND MODELING

J-B. Clavaud [(*)] and J. LaVigne [(**)]
[(*)] Schlumberger Doll Research, CT, USA
[(**)] Schlumberger Well Services, TX, USA

This paper was prepared for presentation at the International Symposium of the Society of Core Analysts held in Pau, France, 21-24 September 2003

ABSTRACT

In this paper, anisotropy of resistivity of thin-bedded formation is investigated experimentally and numerically. The experiments consist of measurements of anisotropy of resistivity on twin-plugs of laminated cores as a function of oil/water saturation. Our results show a clear increase of the anisotropy of resistivity when S_w decreases. This result demonstrates that anisotropy of resistivity is induced by the difference of saturation between the sand layer (oil bearing) and the fine grain layers (water bearing). Our modeling work was designed to compare the robustness of various equations for estimating water saturation. Four models have been defined: a thinly laminated coarse grain sand, a thinly laminated fine grain sand, a thinly laminated sand-shale and a turbidite. The vertical and horizontal resistivity of each formation is calculated with a dual water model. This anisotropy of resistivity is used to compare the oil content in the original model and the one obtained from various S_w equations. This work demonstrates that the use of resistivity parallel (r_h) and transverse (r_v) to the bedding planes and an accurate volume of fine grain, gives better S_w values than shaly-sand equations when we know only the horizontal resistivity. In addition, a new S_w equation for shaly sandstone, which uses both r_v and r_h but does not require the knowledge of water resistivity, is proposed.

INTRODUCTION

Thinly laminated formations can be significant hydrocarbon reservoirs. Often such formations are anisotropic and exhibit the classical "Low resistivity Pay" [1,2]. Cause of very large anisotropy of resistivity (larger than 3) has been investigated over the last decade and is more likely due to the presence of water bearing thin bed (shale layers for example) and oil bearing sand layers [3,4]. Intrinsic electrical anisotropy of sandstone (fully brine saturated) has been recently measured between 1 and 2, according to Jing *et al.* [5]. However, this cannot be generalized to all sandstone and shale, and further research is needed. We are conducting experimental measurements of anisotropy of resistivity in laminated formation as a function of oil content in order to investigate this behavior.

Additionally, we model four Representative Geological Units (RGU) that are: a coarse grain with very fine grain thin bed sandstone (model 1), a very fine grain with coarse grain thin bed sandstone (model 2), a shale-sand sequence (model 3) and a turbidite (model 4). Using a set of petrophysical properties, we can calculate the apparent anisotropy of resistivity of such formations. From the data generated with the forward modeling, we can test the robustness of various S_w equations. Additionally to the classical Archie and dual water equations, which use horizontal resistivity, three other algorithms that use both the vertical and the horizontal resistivity are investigated.

EXPERIMENTS

Description

Our experiments consist of measurements of anisotropy of resistivity on twin-plugs of laminated cores as a function of oil/water saturation. Twin plugs have been used to measure the vertical and horizontal resistivity. By vertical and horizontal, we mean parallel and perpendicular to the bedding plane. Five formations have been chosen: Two Berea sandstones, one Navajo sandstone, one Cutbank sandstone, and one Lyons sandstone. The basic petrophysical properties such as gas porosity and gas permeability are given in the Table 1. Plugs are cylinder of 38.1 mm diameter and 38.1 mm length. The two Berea sandstones are homogeneous, while the Navajo, the Cutbank and the Lyons sandstone have thin laminations.

De-saturation and Resistivity Measurements

Cores were dried and then saturated with a 0.2 Ω·m NaCl brine under vacuum. We achieve the various saturation steps by a centrifuge technique. Centrifugation is done parallel to the bedding plane. The protocol for the de-saturation was done in order to achieve as much as possible a homogeneous distribution of the fluids [6,7]. After careful reviewing of the various option we have decide to centrifuge for 20 hours in one direction, then 20 hours with the core flipped, and finally 12 hours of equilibration time. Centrifugation was done at various rates with Dodecane oil. Saturation measurements were done through gravimetric technique and NMR T_2 distribution.

Measurements of the resistivity were carried out using an HP4294A impedance-meter using the front four terminals of the device. Measurements were made in a pressure vessel with low confining pressure at a frequency of 100 kHz where electrode polarization and contact impedance are minimized [8,9]. An overall ±10% error was estimated by repeated measurements and a comparison of four and two electrodes measurements. The anisotropy of resistivity, defined here as the ratio between the resistivity perpendicular to the bedding and parallel to the bedding (r_v / r_h), is then measured for the various S_w stages.

Experimental Results

Figure 1 illustrates the dependence of the anisotropy of resistivity on water saturation for the five formations tested. When S_w decreases, the ratio between vertical and horizontal

resistivity increases for the laminated formation (Navajo, Cutbank and Lyons). The highest increase is seen for the Navajo sandstone where the anisotropy of resistivity increases from 1.2 to 3.4 when the water saturation decreases from 100% to 10%. The anisotropy remained constant for the two Berea sandstones that are homogeneous. In addition, we see that the anisotropy appears only when S_w is significantly low (around 30% to 40%).

The variation of the ratio r_v / r_h when S_w decreases is attributed to the differential of saturation between the fine grain layer (water bearing) and the coarse grain layer (oil bearing) [3,4]. This demonstrates that the laminated sandstones are isotropic when the core is close to fully water saturated and become anisotropic when S_w gets closer to irreducible water saturation. This behavior is explained in figure 2. As the capillary pressure increases in the laminated formation, the oil enters the coarse grain layer but not the fine grain layer. Since the layer resistivities are summed in series for the vertical resistivity and in parallel for the horizontal, you have an induced anisotropy. To our knowledge, such induced anisotropy has been observed in some oilfields [10,11], but rarely in the laboratory. We have experimentally proven here, that the cause of this anisotropy is not fundamentally intrinsic but is linked with the fact that the fine grain layers hold the water and the coarse grain layers are filled with oil.

MODELING

Description of the Four Representative Geological Units

For the forward modeling of the anisotropy of resistivity we describe four typical sediment patterns: (1) A thinly laminated coarse grain sand, (2) a thinly laminated fine grain sand, (3) a thinly laminated sand-shale and (4) a turbidite. Each one of those formations is defined by a geometrical and petrophysical set of properties and like a sequence of layers with different grain size and/or mineralogy: coarse grain / medium grain / fine grain / very fine grain / shale (Table 2).

Set of Petrophysical Properties

Each layer type has a typical set of petrophysical properties summarized in Table 3. The sand part (layer 1-2-3-4) is a clean to slightly shaly sandstone with a porosity ranging from 25% to 22%. From the coarse grain layer to the very fine grain layer, the dry clay content is increasing from 2% (percent weight) to 15%. The *CEC* of the dry clay content is chosen equal to 0.3 *meq/g*, which corresponds to a mixture of 66% of illite, 16% of kaolinite and 17% of smectite. The density of the dry clay (r_{dcl}) is 2.73 *g/cc*.

Mixing Laws and conductivity equation

A stack of layers (layer 1 and 2) has average total porosity (F_t), water saturation (S_w) and dry clay content (V_{dcl}) that follow the basic set of equations:

$$f_T = f_1 \cdot f_1 + f_2 \cdot f_2 \tag{1}$$

$$S_w = \frac{f_1 \cdot S_{w1} \cdot f_1 + f_2 \cdot S_{w2} \cdot f_2}{f_t} \tag{2}$$

$$V_{dclt} = f_1 \cdot V_{dcl1} + f_2 \cdot V_{dcl2} \quad (3)$$

Here f_1 and f_2 are the volume fraction of each layer. The mixing laws for the resistivity of a stack of layers are described in terms of series and parallel model. The averaging is consequently a classic arithmetic mean and harmonic mean, which leads to:

$$r_v = f_1 \cdot r_1 + f_2 \cdot r_2 \quad (4)$$

$$r_h = \frac{r_1 \cdot r_2}{f_1 \cdot r_2 + f_2 \cdot r_1} \quad (5)$$

Conductivity equations for shaly sand are abundant in the literature [12, 13, 14, 15]. A review of all of them [16] reveals that more than 19 S_w equations are available for the hydrocarbon zone. We have decide to compute the resistivity of each layer according to the Dual Water model [13]:

$$C_t = f_t^{m_{dw}} S_{wt}^{n} \left[\frac{(S_{wt} - S_{wb}) \times C_{wf} + S_{wb} \times C_{wb}}{S_{wt}} \right]. \quad (6)$$

In this model, m_{dw} is the dual water cementation exponent, n is the saturation exponents, S_{wt} is the total water saturation, S_{wb} is the bound water saturation, C_{wf} the free water conductivity, and C_{wb} the bound water conductivity. We derived the various parameters from the cation exchange capacity (CEC), the volume of dry clay (V_{dcl}), the weight percent of dry clay (W_{dcl}), the clay charge contribution per unit pore volume Q_v, the shalyness factor (y), the wet clay porosity (w_{clp}) and the temperature. The m_{dw} is calculated as follow:

$$m_{dw} = 1.75 + 0.258 \cdot y + 0.20\left(1 - e^{-16.4y}\right) \quad (7)$$

Those parameters are presented in the Table 3. Some parameters are equal for all the layers. For example, temperature is set at 150 degree F, wet clay porosity is set at 0.18 and the conductivity of the bound water is set to 18.73 S/m.

Capillary Pressure Curves

In order to simulate the drainage of our stack of layers we approximate capillary pressure curve for each layers. The function used to fit the capillary pressure curve is

$$S_w = (1 - S_{wirr})\left(\frac{P_b}{P_c}\right)^{1/g} + S_{wirr} \text{ if } P_c > P_b \text{ or } S_w = 1 \text{ if } P_c < P_b \quad (9)$$

In this fit, P_b is the entry pressure, S_{wirr} the irreducible water saturation, S_w the total water saturation and γ the exponent that we fix equal to 2. The values of irreducible water saturation were given in the Table 3 and pressure entry were chosen as follow: 1 (arbitrary unit) for the coarse grain layer, 2 for the medium grain layer, 5 for the fine grain layer, 10 for the very fine grain layer and 20 for the shale.

Inversion of the Data Generated by the Forward Modeling

Models using horizontal resistivity only

One output of the forward modeling is the averaged horizontal resistivity as a function of water saturation S_w, varying from 1 to S_{wirr} for a given set of averaged properties. We

have decided to calculate the water content using Archie and dual water where the input parameters are the averaged values of horizontal resistivity obtained by the forward modeling.

Models using vertical and horizontal resistivity

In a 2001 SPE paper [17], following the work done by Klein et al [3, 4], F. Shray, proposed an algorithm for water saturation computation in thin-bedded formations, where the inputs are the horizontal resistivity, the vertical resistivity, the fine grained volumetric fraction (from NMR) and the water resistivity. We will refer to the model by the acronym SPC. In this approach, the thin-bed is seen as a bi-modal system composed of coarse grain layers and fine grain layers. Knowing the horizontal and vertical resistivity, the amount of fine grain material you first calculate the resistivity of the coarse grain and fine grain layer. Then you calculate the amount of water in each layer using Archie's law (with m and n equals to 2), then the total amount of water (S_{wSPC}).

Another approach, which is closely related to the previous one, uses dual water model to invert the water saturation of the layers instead of a simple Archie's law. We will refer to the model by the acronym HDA. This leads to the following equation for water saturation in each layer if we assume a saturation exponent n equal to 2:

$$S_{wHDA} = S_{wb} \times \frac{\left(C_{wf} - C_{wb}\right)}{2\,C_{wf}} + \frac{\sqrt{4\,C_t\,C_{wf}\,f_t^{\,m} + \left[\left(C_{wf} - C_{wb}\right) \times S_{wb}\,f_t^{\,m}\right]^2}}{2\,C_{wf}\,f_t^{\,m}} \qquad (10)$$

In this approach we need to know the conductivity of the layer C_t, the one of the free water C_{wf} and bound water C_{wb}, the bound water saturation S_{wb} the total porosity F_t, and the Dual Water cementation exponent m_{dw} (Equation 7). In this model, we have used a bound water conductivity of 18.7 *S/m*.

The two previous models use for input parameters the water resistivity and are multi-steps models. We describe an algorithm that allows us a direct computation of S_w from the vertical and horizontal resistivity only. The range of application for this model is limited to system where the thin bed layers have irreducible water saturation equal to 1. The model assumes first that the system is a bi-modal system composed of coarse grain layer and fine grain layer only. The second hypothesis is that the resistivity of the two layers follows an Archie's law, each layer is isotropic and that the water resistivity is the same in both layers. We can consequently write:

$$r_{cg} = r_w \cdot f_{cg}^{-m_{cg}} \cdot S_{wcg}^{-n_{cg}} \qquad (12)$$

$$r_{fg} = r_w \cdot f_{fg}^{-m_{fg}} \cdot S_{wfg}^{-n_{fg}} \qquad (13)$$

We know that the vertical and horizontal resistivities of a layered system are calculated using equations 4 and 5. If know we assume that both the cementation and saturation exponent of both layers are equal to 2, the ratio between the horizontal and vertical resistivity is:

$$\frac{r_v}{r_h}=1-2f_{fg}+2f_{fg}^2+f_{fg}\cdot\frac{S_{wcg}^2\cdot f_{cg}^2}{S_{wfg}^2\cdot f_{fg}^2}-f_{fg}^2\cdot\frac{S_{wcg}^2\cdot f_{cg}^2}{S_{wfg}^2\cdot f_{fg}^2}+f_{fg}\cdot\frac{S_{wfg}^2\cdot f_{fg}^2}{S_{wcg}^2\cdot f_{cg}^2}-f_{fg}^2\cdot\frac{S_{wfg}^2\cdot f_{fg}^2}{S_{wcg}^2\cdot f_{cg}^2} \quad (14)$$

If we say that the fine layer is fully saturated with brine ($S_{wfg} = 1$), then we can rewrite the porosity and saturation of the coarse grain layer as functions of the bulk properties and the fine grain properties:

$$f_{cg}=\frac{f_T-f_{fg}\cdot f_{fg}}{f_{cg}} \quad (15)$$

$$S_{wcg}=\frac{f_t\cdot S_{wt}-f_{fg}\cdot S_{wfg}\cdot f_{fg}}{f_{cg}\cdot f_{cg}}=\frac{f_t\cdot S_{wt}-f_{fg}\cdot f_{fg}}{f_{cg}\cdot f_{cg}} \quad (16)$$

If we assume that the fine grain layer porosity and the total bulk porosity of the stack are very close ($F_{fg} @ F_t$), then the anisotropy of resistivity can be expressed like:

$$\frac{r_v}{r_h}=1+\frac{2f_{fg}-4f_{fg}^2+f_{fg}^3}{f_{fg}-1}+\frac{2\cdot f_{fg}^2}{f_{fg}-1}S_{wt}-\frac{f_{fg}}{f_{fg}-1}S_{wt}^2+\frac{f_{fg}-3f_{fg}^2+3f_{fg}^3-f_{fg}^4}{\left(S_{wt}-f_{fg}\right)^2} \quad (17)$$

The general form of this equation is:

$$\frac{r_v}{r_h}=1+a+bS_{wt}+cS_{wt}^2+\frac{d}{\left(S_{wt}-e\right)^2} \quad (18)$$

After an analysis of sensitivity, we conclude that only the terms associated with the constant a, d and e are important, at least when we are close to the irreducible saturation:

$$\frac{r_v}{r_h}=1+\frac{2f_{fg}-4f_{fg}^2+f_{fg}^3}{f_{fg}-1}+\frac{f_{fg}-3f_{fg}^2+3f_{fg}^3-f_{fg}^4}{\left(S_{wt}-f_{fg}\right)^2} \quad (19)$$

It is now easy to invert the ratio r_v / r_h to get S_{wt}:

$$S_{wt}=S_{wSDR}=\left[\frac{f_{fg}-3f_{fg}^2+3f_{fg}^3-f_{fg}^4}{\frac{r_v}{r_h}-1-\frac{2f_{fg}-4f_{fg}^2+f_{fg}^3}{f_{fg}-1}}\right]^{1/2}+f_{fg} \quad (20)$$

We will refer to the model by the acronym SDR.

Comparison Between Forward Models and S_w Equations

Initial parameters

For each of the four system modeled here, we have decide to test two different salinities; a fresh brine (0.1 Ω·m) and more salty brine (0.03 Ω·m). For the shale-sand model, we also decide to make the amount of fine grain material or shale material flexible from 10% to 30 %. The difference between the computed values and the initial value of the forward modeling for the bulk volume of hydrocarbon (BVH) is noted DHC_{xxx}. This value is the difference in percent between the BVH_{XXX} of the model "XXX" and the input, BVH_t, of the forward modeling

Model 1: Coarse grain thick layer / Fine grain thin bed

This model is a stack of coarse grain sand (low S_{wirr}) and fine grain sand (high S_{wirr}). We did not test the SDR equation on this model, because the SDR equation assumes that S_{wirr} is equal to one in the fine grain layer. We have tested this model with a fraction of fine grain material equal to 0.3 and two salinities: 0.1 Ω·m and 0.3 Ω·m. The Results for the low salinity case is presented in the Figure 3. The Tables 4 and 5 give the detail of the computation results. For both the high and low salinity, Archie and DW quite over estimate the water content. However, the two algorithms (SPC and HDA) that are using both the vertical and the horizontal resistivity, give much better results. If we now look at the bulk volume of hydrocarbon in the formation things are, as expected, in favor of the r_v / r_h approach. For example, at low salinity the SPC and HDA algorithms give a bulk volume of hydrocarbon respectively equal to 0.172 and 0.182, while Archie leads to a value of 0.143 (initial value = 0.179). This increase in the reserve (about 25% more oil in place) might make a big difference when considering the economical value of such a formation.

Model 2: Fine grain thick layer / Coarse grain thin bed

This model leads to different result at low and high salinity (Table 4 and 5). In one hand, for the low salinity situation all the models, but HDA, tested fail to give accurate values for the bulk volume of hydrocarbon (around -16% to –35% of difference). On the other hand, at high salinity, SPC and HDA equations seem to work better. However, those discrepancies are just reflecting the small amount of oil in the formation.

Model 3: Laminated Sand-Shale

This model is a thinly laminated high resistivity sand and low resistivity shale. In this case, we have tested the three algorithms (SPC, HDA and SDR). The use of SDR algorithm is justified here by the fact that the shale layer has an irreducible water saturation of 100%. The results for this model are presented for the two cases (low salinity and high salinity) and for two different shale contents (10% and 30%).

From the result of our simulation (Figures 4), we can say that Archie and DW models that use only the horizontal resistivity give too low oil content. When we compare with the three algorithms that use both the vertical and the horizontal resistivity, we see a much better agreement for the bulk volume of hydrocarbon. The HDA and SPC equations work well in all cases but the low salinity and 30% shale seems to be more challenging. For this sand-shale system, it is noticeable that those models (SPC, HDA and SDR) slightly over estimate the amount of oil. Nonetheless the bulk volume of oil computed by those three algorithms are much more accurate than the simple Archie or even DW model. However, the differences between the three algorithms are small (around 4% at S_{wirr}). The results are summarized in the Tables 4 and 5. From our work, we can say that for the sand shale sequence, the three algorithms are suitable and choosing one rather than the others relies on your knowledge of the formation. If you have access to a lot of information, included bound water saturation then you best choice is HDA, if you have

only access to the water conductivity the SPC is you best pick, and if you have no knowledge about formation water resistivity the SDR equation is the one to use.

Model 4: Turbidite

The turbidite model is of a great interest for the oil industry because of the widespread of such reservoir type in the deep offshore business [18]. Again, the S_w values computed from the algorithm that use both the vertical and the horizontal resistivity are in much better agreement with the forward model inputs (Figure 5). In one hand, all three algorithms (SDR, SPC, HDA) give good results. On the other hand, the SDR and HDA algorithms seem to be less sensitive to the salinity (Tables 4 and 5).

Application to Experimental Data

Our set of data being mainly eolian sandstone only the SPC equation has been tested for the laminated formations. The amount of grain material was computed from the NMR T_2 distribution of the samples. We have chosen a 33 ms cutoff [19]. Results are presented in the Table 6 for the three laminated formations and for two water saturations. We can see that the use of only the horizontal resistivity and Archie's law leads to too much water. However, the SPC model that uses both vertical and horizontal resistivity give water saturation in much better agreement with bulk value measured by buoyancy. We see also that the SPC model tends to overestimate oil content. This has been shown also with the modeling developed above. One has to note that the anisotropy measured are much smaller than the anisotropy modeled in this work. One obvious reason is that our samples are eolian sandstones where it's more likely that the water saturation in the thin lamination is not close to one. Another factor is the fact that the amount of lamination is small in our sample set.

CONCLUSION

A set of anisotropy of resistivity experiment was achieved. In this experiment, twin plugs of laminated and non-laminated formations were measured. For different water saturation, we have measured the vertical and horizontal resistivity. We found that the ratio of the vertical and horizontal resistivity increases when bulk water saturation decreases in laminated formation. For non-laminated formations (i.e. homogeneous), we found that the anisotropy of resistivity remains constant and close to one regardless of the bulk water saturation. The change of the ratio r_v / r_h when S_w decreases is attributed to the differential of saturation between the fine grain layer (water bearing) and the coarse grain layer (oil bearing). This demonstrates that the laminated sandstones are isotropic when the core is close to fully water saturated and become anisotropic when S_w gets closer to irreducible water saturation. We have experimentally proven here, that the cause of this anisotropy is not fundamentally intrinsic but is linked with the fact that at irreducible bulk water saturation, the fine grain layers hold the water and the coarse grain layers are filled with oil. Using forward modeling, we have computed the anisotropy of resistivity of four Representative Geological Unit (thick layers of coarse sand with thin layers of very fine sand / thick layers of fine sand with thick layers of coarse sand, thinly

laminated sand-shale and turbidite). From a given set of petrophysical parameters (porosity, irreducible water saturation, CEC and dry clay content), a Dual Water (DW) equation was used to generate the resistivity of each layer. The output of this forward modeling is the vertical and horizontal resistivity, the total porosity and shale content. From this output, we have computed the water saturation from the horizontal resistivity using Archie and DW and from both the vertical and horizontal resistivity using three algorithms (SPC, HDA and SDR).

In one hand, we have found that the turbidite model is well characterized by the SDR equation, that the sand-shale model can be assessed through the SPC and HDA and in some extent by the SDR equation. On the other hand, the model number one (fine grain thin layers between coarse grain tick sand bodies) requires the SPC or HDA algorithm for evaluation. The main difference between the SPC and HDA algorithms in one side and the SDR equation in the other side is the knowledge of water resistivity and the fact that SDR equation is a single step algorithm while the others requires four steps of computation. For the thinly laminated sand-shale sequence and turbidite at irreducible water saturation, the SDR equation is a potential candidate for a quick answer at the well site, while the SPC and HDA algorithm are good candidates for more complex answer. For the grain size variation problem the SDR equation is not useful (because of the 100% water saturation in the fine grain assumption) and we have to rely on the SPC or HDA equation. However, the SPC has the advantages of requiring less data, particularly the bound water saturation and the water conductivity. As a conclusion, we can say that the use of 3D resistivity measurement combined with a fine grained fraction measurement (NMR or Gamma Ray) can provide a good thin-bed evaluation methodology, and increase significantly the value of thin-bedded reservoirs.

REFERENCES

[1] Boyd, A., Darling, H., Tabanou, J., Davis, B., Lyon, B. Flaum, C., Klein, J., Sneider, R.M., Sibbit A. and Singer, J., The lowdown on low-resistivity pay, *Oilfield Review*, 1995, **Autumn**, pp. 4-18.

[2] Worthington, P.F., Recognition and evaluation of low resistivity pay, *Petroleum Geoscience*, 2000, **6**, pp 77-92,.

[3] Klein, J.D., Saturation effects on electrical anisotropy, *The log Analyst*, 1996, **January.-February**, pp. 47-49.

[4] Klein, J.D., Martin, P.R. and Allen, D.F., The petrophysics of electrically anisotropic reservoirs, *The Log Analyst*, **May-June.**, 1997.

[5] Jing, X.D., Al-Harthy, S. and King, S., Petrophysical Properties and Anisotropy of Sandstones under True-Triaxial Stress Conditions, *Petrophysics*, **43**, Jul.-Aug. 2002, pp358-364.

[6] Baardsen, H., Nilsen, V. Leknes, J. and Hove, A., Quatifying saturation distribution and capillary pressures using centrifuge and computer tomography, *in Reservoir Characterization II*, Academic Press, 1991, pp. 102-121.

[7] Ruth, D.W. and Chen, Z. A., Measurement and interpretation of centrifuge capillary pressure curves-The SCA curvey data, *The log Analys.*, **September.-October.** 1995, pp. 21-33.

[8] Garrouch, A. A., A systematic study revealing resistivity dispersion in porous media, *The*

Log Analyst, 1999, **July-August**, pp. 271-279.
[9] Garrouch A. A., and Sharma M. M., The influence of clay content, salinity, stress, and wettability on the dielectric properties of brine-saturated rocks: 10 Hz to 10 MHz, *Geophysics*, 1994, **59**, pp. 909-917.
[10] Page, G.C., Fanini, O.N., Kriegshauser, B.F., Mollisonm R.A., Yu, L. and Colley, N., Field example demonstrating a significant increase in calculated gas-in-place: An enhanced shaly sand reservoir characterisation model utilizing 3DEX™ multicomponent induction data, *SPE* 71724, 2001.
[11] Yu, L., Fanini, O.N. Kriegshhauser, B.F. Koelman, J.M.V. and Van Popta, J., enhanced evaluation of low resistivity reservoir using multi-component induction Log Data, *Petrophysics*, 2001, **42**, pp. 611-623.
[12] Waxman, M.H. and Smits, L.J.M., Electrical conductivities in oil-bearing shaly sands, *SPE J.* , 1968, **8**, pp. 107-382.
[13] Clavier, C., Coates G. and Dumanoir, J., Theoritical and experimental bases for the dual-water model for interpretation of shaly sands, *SPE J.* , 1984, **24**, pp. 153-168.
[14] Sen, P.N., Good, P.A. and Sibbit, A., Electrical conduction in clay bearing sandstones at low and high salinities, *J. Appl. Phys.*, 1988, **63**, pp. 44832-4840.
[15] Revil, A., Cathles III, L.M., Losh, S. and Nunn, J.A., Electrical conductivity in shaly sands with geophysical applications, *J. Geophys. Res.*, 1998, **103**, pp. 23,925-23,936.
[16] Worthington, P.F., The evolution of shaly-sand concepts in reservoir evaluation, *The Log Analyst*, 1985, **26**, pp. 23-40.
[17] Shray, F. and Borbas, T., Evaluation of laminated formations using nuclear magnetic resonance and resistivity anisotropy measurements, *SPE* 72370, 2001.
[18] Dromgoole, P., Bowman M., Leonard, A., Weimer, P. and Slatt, R.M., Developing and managing turbidite reservoirs – case histories and experiences: results of the 1998 EAGE/AAPG research conference, *Petroleum Geosciences*, 2000, **6**, pp. 97-105.
[19] Matteson, A., Tomanic, J.P., Herron, M.M., Allen, F.F. and Kenyon, W.E., Relaxation of clay-brine mixtures, *SPE* 49008, 1998.

Table 1. Petrophysical properties of the five formations tested.

Sample name	Axe	Porosity	k (mD)	Description
B100-V	Vertical	0.18	90	Homogeneous Berea sandstone
B100-H	Horizontal	0.18	120	Homogeneous Berea sandstone
B500-V	Vertical	0.23	900	Homogeneous Berea sandstone
B500-H	Horizontal	0.23	750	Homogeneous Berea sandstone
NAV-V	Vertical	0.13	900	Laminated Navajo sandstone
NAV-H	Horizontal	0.14	30	Laminated Navajo sandstone
CB-V	Vertical	0.15	5	Laminated Cutbank sandstone
CB-H	Horizontal	0.15	0.5	Laminated Cutbank sandstone
L266-V	Vertical	0.15	1150	Laminated Lyons sandstone
L266-H	Horizontal	0.15	150	Laminated Lyons sandstone

Table 2. Proportion of each layer type in the four models (volume fraction).

Model	Description	Layer 1 Coarse	Layer 2 Medium	Layer 3 Fine	Layer 4 Very fine	Layer 5 Shale
1	Coarse grain sediment with layers of very fine grain material	70%	0%	0%	30%	0%
2	Very fine grain sediment with layers of coarse grain material	20%	0%	0%	80%	0%

3	Sand-shale thin-bed sediment	70%	0%	0%	0%	30%
4	Turbidite (fining up)	25%	25%	20%	20%	10%

Table 3. Petrophysical prope rties and dual water parameters of the various layers.

Type	Φ	S_{wirr}	S_{wb}	W_{Clay}	W_{dcl}	V_{dcl}	F	Q_v	S_{wb}	y	m_{dw}
Coarse	25 %	8%	2%	2%	2%	1.5%	12	0.05	1.3%	0.016	1.80
Medium	23%	20%	3%	5%	5%	4%	16	0.13	3.5%	0.040	1.86
Fine	22%	40%	4%	10%	10%	8%	21	0.28	7.5%	0.080	1.92
Very Fine	22%	80%	8%	15%	15%	12%	23	0.42	11.3%	0.119	1.95
Shale	30%	100%	60%	60%	60%	42%	21	1.13	30.1%	0.486	2.08

Table 4. Results of the inversion (saturation) for the model number 1 to 4.

Mod.	f_{fg}	r_w (Ω.m)	r_v (Ω.m)	r_h (Ω.m)	r_v / r_h	S_{wt}	S_{wt} Archie	S_{wt} WS	S_{wt} SPC	S_{wt} HDA	S_{wt} SDR
1	0.3	0.1	270	8.8	30.7	26%	44%	39%	29%	25%	-
1	0.3	0.03	110	3.1	35	26%	40%	38%	26%	25%	-
2	0.8	0.1	78.9	3.3	23.7	63%	77%	69%	70%	63%	-
2	0.8	0.03	32.2	1.2	26.9	63%	70%	69%	64%	63%	-
3	0.1	0.1	345	9.4	37	16%	40%	36%	16%	14%	15%
3	0.3	0.1	269	3.2	42	37%	67%	61%	34%	32%	34%
3	0.1	0.03	142	4.1	35	16%	34%	32%	15%	15%	15%
3	0.3	0.03	110	1.4	79	37%	55%	57%	34%	36%	34%
4	0.1	0.1	112	5	23	40%	60%	54%	37%	35%	37%
4	0.3	0.03	46	2	24	40%	52%	52%	35%	35%	37%

Table 5. Results of the inversion (BVH) for the model number 1 to 4.

Mod.	f_{fg}	r_w Ω.m	BVH_t	BVH_t *Arch.*	BVH_t *DW*	BVH_t *SPC*	BVH_t *HDA*	BVH_t *SDR*	*DHC Arch.*	*DHC DW*	*DHC SPC*	*DHC HDA*	*DHC SDR*
1	0.3	0.1	0.179	0.134	0.158	0.172	0.182	-	-25%	-17%	-4%	2%	-
1	0.3	0.03	0.179	0.143	0.150	0.178	0.182	-	-20%	-16%	-1%	2%	-
2	0.8	0.1	0.082	0.053	0.069	0.068	0.084	-	-35%	-16%	-17%	2%	-
2	0.8	0.03	0.082	0.068	0.071	0.082	0.084	-	-17%	-13%	-1%	2%	-
3	0.1	0.1	0.214	0.152	0.164	0.215	0.220	0.218	-29%	-23%	1%	3%	2%
3	0.3	0.1	0.166	0.088	0.104	0.174	0.180	0.176	-47%	-37%	5%	8%	6%
3	0.1	0.03	0.214	0.170	0.173	0.217	0.216	0.218	-21%	-19%	2%	1%	2%
3	0.3	0.03	0.166	0.118	0.114	0.176	0.171	0.176	-29%	-31%	6%	3%	6%
4	0.1	0.1	0.143	0.095	0.110	0.149	0.155	0.150	-33%	-23%	4%	8%	5%
4	0.1	0.03	0.143	0.114	0.115	0.156	0.155	0.150	-20%	-20%	9%	8%	5%

Table 6. Comparison between measured S_w and computed S_w for the Archie's law and the SPC algorithm.

Sample	r_v / r_h	Sw bulk	Sw Archie	Sw SPC
NAV	2.5	0.21	0.27	0.22
NAV	3.3	0.12	0.17	0.13
L266	1.7	0.20	0.32	0.21
L266	1.8	0.14	0.24	0.16
CB	1.7	0.60	0.67	0.55
CB	2.5	0.45	0.57	0. 41

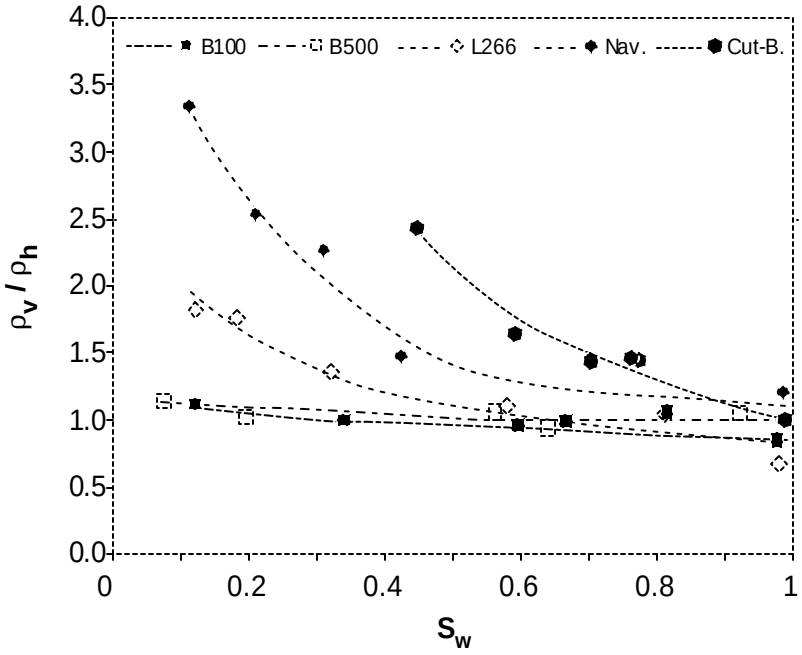

Figure 1: Ratio between vertical and horizontal resistivity versus bulk water saturation.

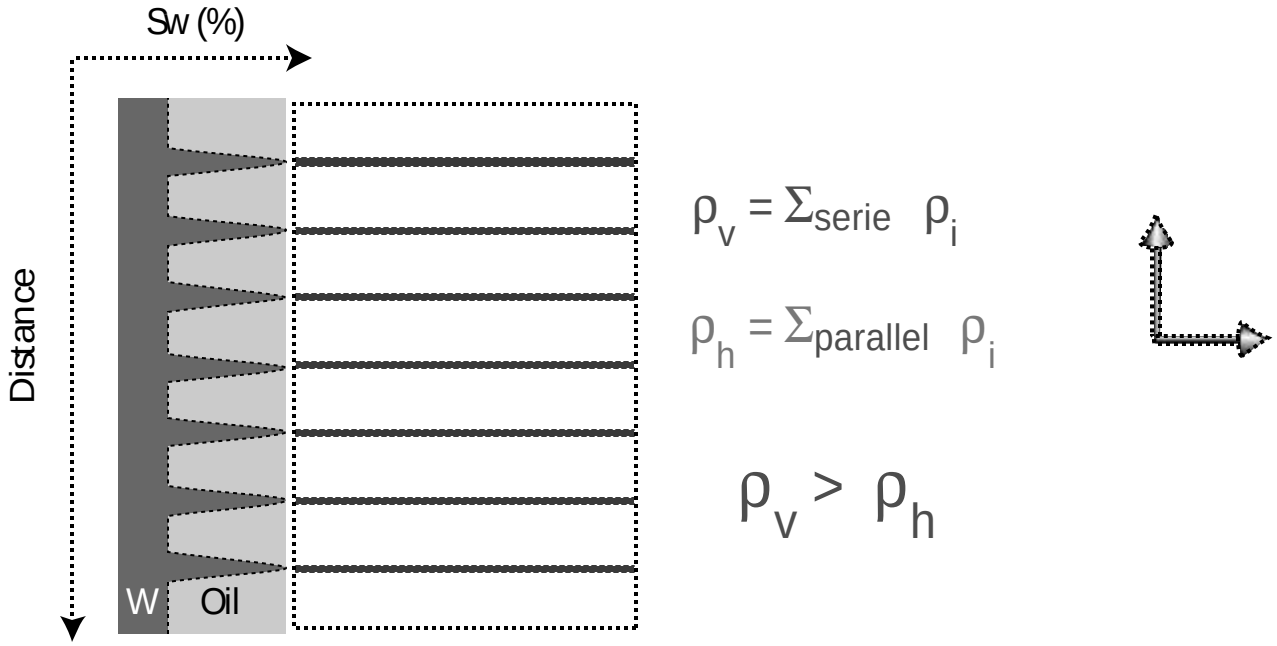

Figure 2: Anisotropy of resitivity in laminated formation.

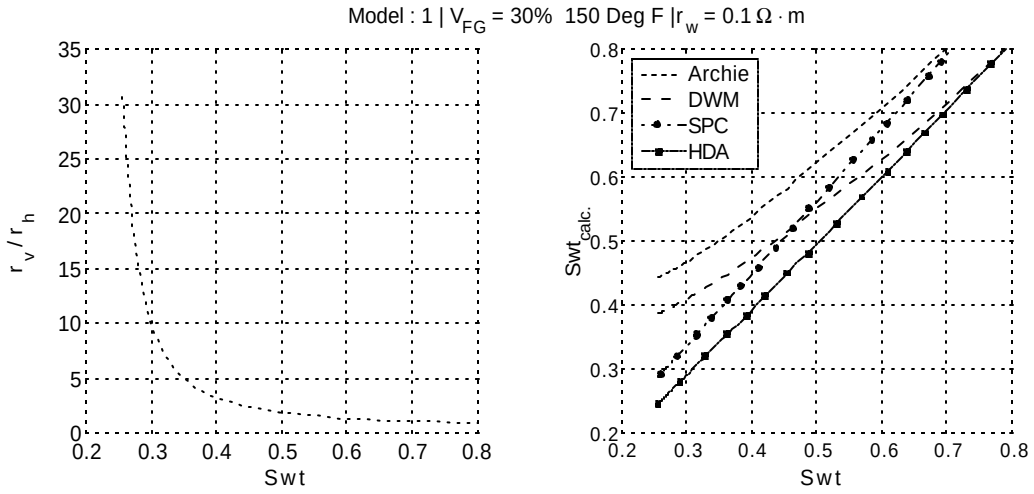

Figure 3: Anisotropy or resistivity and water saturation comparison for the model 1

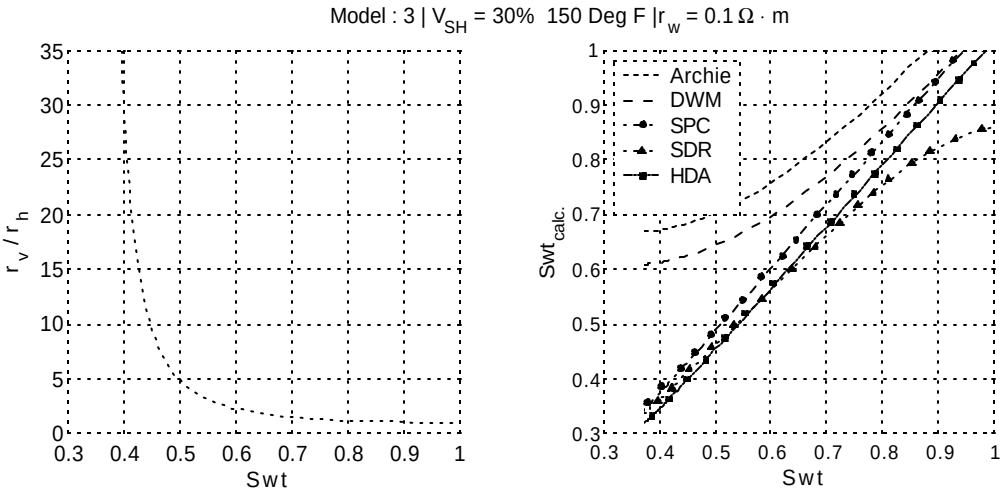

Figure 4: Anisotropy or resistivity and water saturation comparison for the model 3

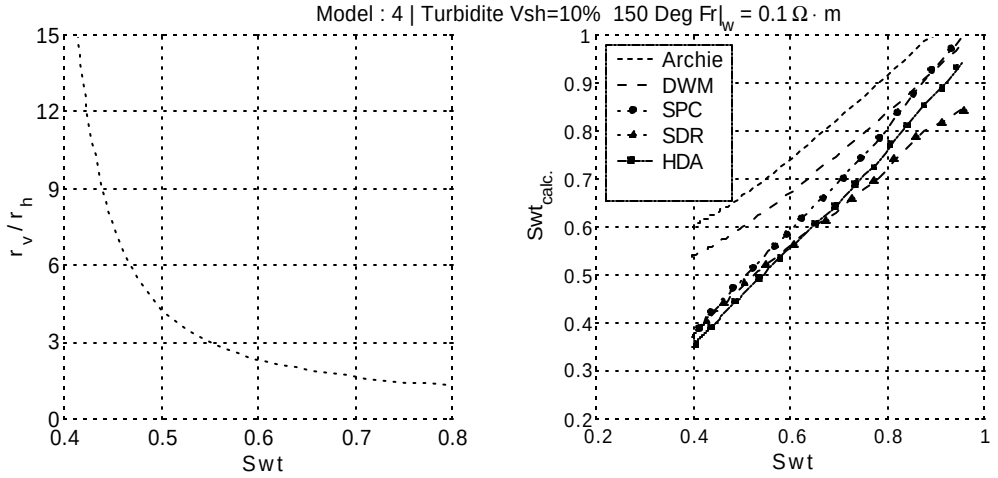

Figure 5: Anisotropy or resistivity and water saturation comparison for the model 4